ARTICLE

Selective Tuning and Optimization of the Contacts to Metallic and Semiconducting Single-Walled Carbon Nanotubes

Peter N. Nirmalraj and John J. Boland*

School of Chemistry and Center for Research on Adaptive Nanostructures and Nanodevices (CRANN), Trinity College Dublin, Dublin 2, Ireland

ABSTRACT Conductance imaging atomic force microscopy was used to probe the electrical interface between single-walled carbon nanotubes and metal electrodes. The contact resistance was optimized by applying a local voltage pulse (~2 s) using a conductive probe with controlled loading force to the region of the metal electrode contacting the nanotube. Using this technique, we show that Pd forms superior contacts, resulting in contact resistance values that are among the lowest ever reported.

KEYWORDS: single-walled carbon nanotubes (SWCNTs) · conductance imaging atomic force microscopy (CI-AFM) · contact resistance

The electrical interface between single-walled carbon nanotubes (SWCNTs) and metal electrodes has been an area of intense research in recent years. In particular, Schottky barriers are known to exist whenever electrical contact is established between a semiconducting nanotube and a metal, which arises because of charge transfer between the SWCNT and the contact metal. The presence of such barriers is a major obstacle to the use of these materials in electronics applications, and so inherently attractive properties of SWCNTs, such as ballistic conduction,[1,2] cannot be easily exploited. In the design of any one-dimensional device structure using SWCNTs, it is essential to understand the origins of Schottky barriers and to develop strategies to minimize their influence in order to attain the quantum conductance limits of a one-dimensional system ($h/4e^2 \sim 6.5$ kΩ).

Different metals ranging from Pd,[1,3] Pt,[4] Sc,[5] Y,[6] and Ti[7] have been investigated as potential contact materials to SWCNTs. Quantum mechanical density functional calculations have suggested that Ti can form ohmic contacts with both metallic and semiconducting tubes due to the formation of strong chemical bonds with the carbon atoms. However, Ti is known to easily oxidize on exposure to air such that these contacts tend to degrade over time. On the other hand, Pd in particular has been shown to eliminate the contact barriers with semiconducting nanotubes due to its high work function and excellent wetting interactions with the nanotubes.[2]

Numerous strategies have been described in the literature to optimize and evaluate the properties of the contacts between SWNTs and metals. Rapid thermal annealing,[8] electroless metal deposition,[9] ultrasonic nanowelding,[10] electrical stressing,[11] and joule heating[12,13] have been performed in order to minimize the contact resistance between the metal of choice and the nanotube. Rapid thermal annealing subjects the entire substrate to the high-temperature annealing, whereas ultrasonic welding can cause serious damage to the pristine nanotube structure. Moreover, techniques like electroless metal deposition are complicated and cannot be readily applied in large-scale fabrication. Joule heating studies by Dong *et al.*[12] report the need for several pulsing voltage sweeps to reduce the contact resistance between the nanotube and the metal electrode, which can result in the separation of some tubes from the metal electrode and can actually result in an increased contact resistance. Here, we study the behavior of metallic and semiconducting nanotubes using conductance imaging atomic force microscopy (CI-AFM)[14−16] and present a simple procedure to tune and optimize the contact resistance of SWCNTs with two of the widely used metal electrodes: Pd and Ti/Au. This is a controlled optimization process that is straightforward yet results in

*Address correspondence to jboland@tcd.ie.

Received for review March 3, 2010 and accepted June 14, 2010.

Published online June 18, 2010.
10.1021/nn100432f

© 2010 American Chemical Society

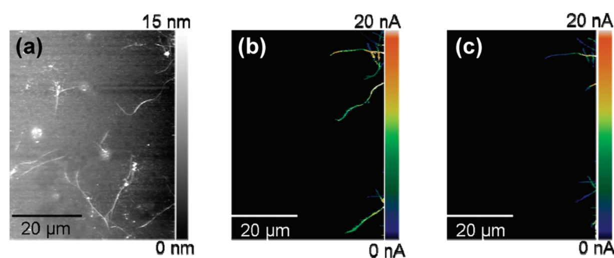

Figure 1. Selective analysis of metallic and semiconducting tubes *via* applying a gate voltage. (a) Topography of a random nanotube network connected to the electrode on the right (not shown in the image). (b) Current map of the same network on applying a bias voltage of 5 mV. The tubes that are connected to the electrode turn on after applying a bias voltage,thereby highlighting the tubes that are electrically well-connected to the network. (c) On applying a gate voltage of +2 V, the semiconducting tubes are turned off and only the metallic species are visible in the current map. After turning off the gate voltage, the current conduction is restored in the semiconducting tubes. To start with, we carefully analyzed individual tubes connected to Ti/Au electrodes.

contact resistances that are among the lowest ever reported.

RESULTS AND DISCUSSION

Individual and isolated SWCNTs were first located by AFM in tapping mode, and the diameter of the tube was verified to be 1.2−1.8 nm. Note that only individual tubes were considered here as SWCNT bundles (identified by their large diameters) contain mixtures of metallic and semiconducting tubes that complicate the analysis. Once an individual tube was located close to the electrode, the AFM was switched to the CI-AFM mode and a very small bias (0.5−5 mV) was applied to the electrode to check the electrical connectivity between the electrode and the nanotube. After verifying that the nanotube was conductive, a gate voltage of ∼+2 V was applied, which rendered the semiconducting tubes nonconducting due to their intrinsic p-doping, and thus allowing CI-AFM to exclusively image the metallic tubes.[16]

In this manner, we can selectively analyze metallic and semiconducting tubes within a random network, as shown in the backgating experiment in Figure 1. Figure 2a shows a typical example of a metallic tube (tube diameter = 1.65 nm) attached to a Ti/Au electrode. By tracing the current map along the length of the well-resolved nanotube (black trace, Figure 2b), it is possible to estimate the resistivity of the tube itself and the resistance at zero length provides an estimate of the contact resistance due to the leads. The resistivity (ρ) can be calculated from eq 1, where $R(d)$ is the measured resistance at any point d along the length of the tube, R_c is the contact resistance, and A is the cross-sectional area of the tube calculated from its measured diameter assuming a cylindrical shape.

$$R(d) = R_c + \rho(d/A) \quad (1)$$

Using this equation, we calculate the resistivity of the pristine metallic tube connected to the Ti/Au electrode in Figure 2a to be 1.41×10^{-8} Ωm and the diameter of the tube is measured to be 1.65 nm based on the topographic analysis. This resistivity compared favorably with resistivity values of those previously reported by Li *et al.*[17] (tube diameter = ∼3 nm).

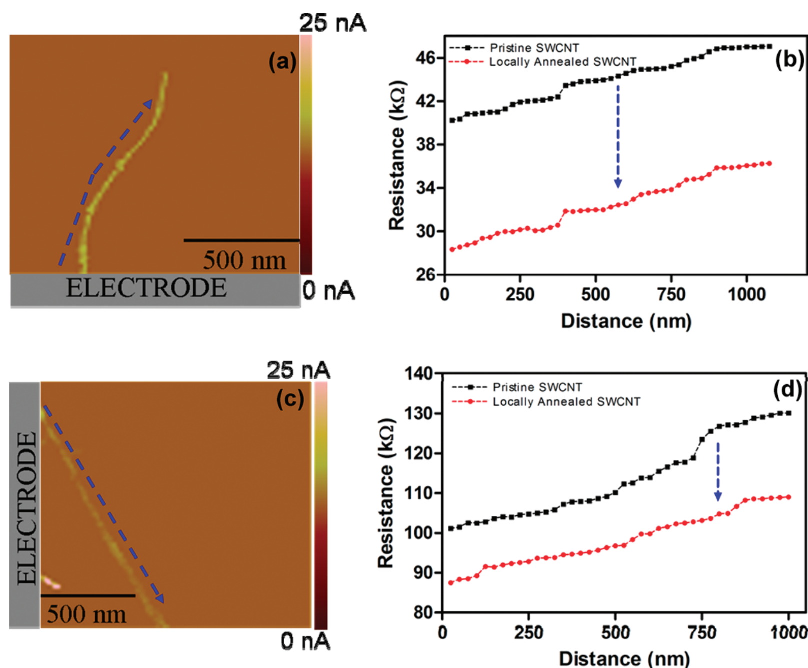

Figure 2. Contact resistance analysis of metallic and semiconducting SWCNTs contacted to Ti/Au electrodes. (a,c) Current map of an individual metallic and semiconducting tube connected to the electrode. (b,d) Analysis of the contact resistance of the pristine tube (black trace) and the same tube after subjecting to local annealing (red trace) by applying 6 V to the Ti/Au electrode next to the respective tubes. The contact resistance was observed to drop after application of a single pulse (scanning conditions, V_{bias} = 2 mV; preamplifier sensitivity, 100 nA/V).

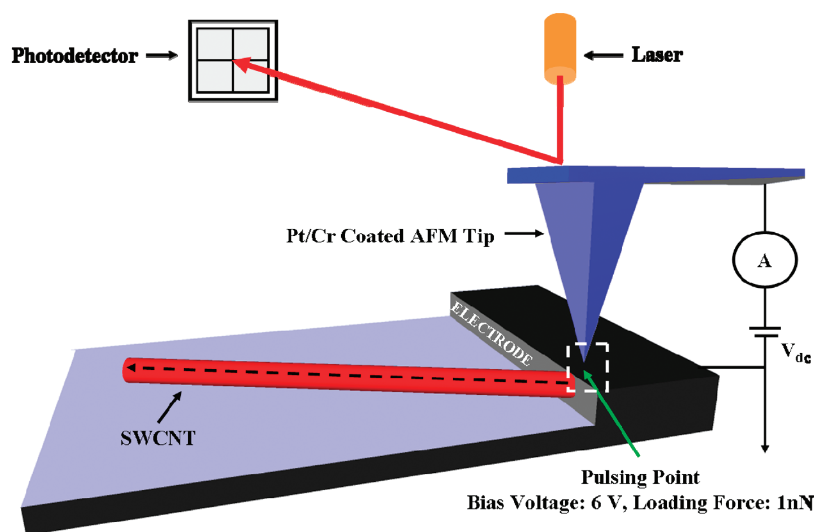

Figure 3. Schematics for the local pulsed annealing experimental setup. The metal-coated tip is biased through which a voltage is applied locally over the electrode on the surface close to the region where the nanotube is located. The loading force and voltage applied between the tip and sample is crucial in reducing the overall contact resistance of the nanotube connected to the metal electrode.

The intercept in the data in Figure 2b reveals a contact resistance at the Ti/Au electrode of 40.2 kΩ. This is an exceptionally low contact resistance, demonstrating that contact processing and solvent removal is very effective when compared to previous values of about 100 kΩ reported for Ti/Au metallic nanotube contacts.[18,19] Likewise, we can calculate the resistivity and contact resistance for the semiconducting nanotube (tube diameter = 1.6 nm) in Figure 2c connected to the same Ti/Au electrode, to yield values of 6.64×10^{-8} Ωm and 96.86 kΩ (calculated from black trace of Figure 2d), respectively, both of which are larger than that found for the case of metal SWCNTs but comparable to the best values ever reported for semiconducting tubes.

To further improve the contact resistance between the metal electrode and the nanotube, we applied a controlled voltage pulse using the AFM tip to the region of the electrode where the SWCNT is connected. A schematic detailing the experimental process is shown in Figure 3. This treatment is expected to produce local heating that might help optimize the contact resistance with the electrode. With a 6 V bias applied to the AFM tip, we used the "point and shoot" capability of our AFM system to position the tip on the electrode at the location where the nanotube was connected. After applying a quick pulse, the tip was withdrawn and re-engaged in contact mode. The AFM tip was set at ground potential and a low bias of 2 mV applied to the nanotubes through the Ti/Au electrode and the resistances are shown by the red traces in Figure 2b,d. As a result of this 6 V pulsing procedure, the contact resistance of the metallic tube was found to decrease by ~12 kΩ, whereas the resistivity or the slope of the current trace remained essentially unchanged. Similar measurements were performed on individual semiconducting tubes connected to the Ti/Au electrode, as shown in the current map (Figure 2c). After pulsing, the contact resistance between the tube and Ti/Au was found to decrease by ~10 kΩ (red trace of Figure 2d). On the basis of these results, it is clear that it should be possible to tune the contact resistance by controlling the magnitude or the duration of the pulse.

Figure 4a shows the results of a systematic study in which the effect of the magnitude of the voltage pulse was studied for a metallic tube (shown in Figure 2a) connected to a Ti/Au electrode. The resistance was observed to gradually decrease as the pulse voltage was increased from 1 to 6.5 V. Above 6 V, the contact resistance was observed to saturate, and applying more than 7.5 V, led to the disintegration of the tube. Similar results were also observed for semiconducting tubes; except that in each case the saturation level of the contact resistance was higher than that observed for metallic tubes. After each voltage pulse, the resistance val-

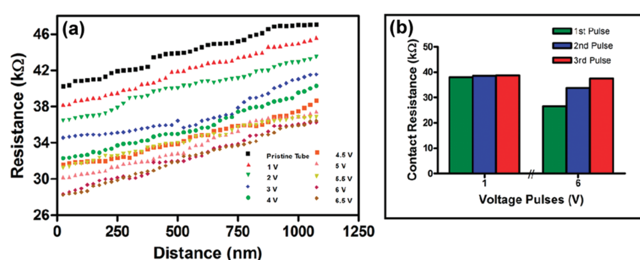

Figure 4. (a) Analysis of the contact resistance along a metallic SWCNT connected to a Ti/Au electrode. The resistance is observed to decrease in steps from ~40 to ~28 kΩ as the pulsing voltage is increased from 1 to 6.5 V, after which the effect was observed to saturate. All of the resistance traces were recorded at a constant bias voltage of 2 mV after the application of the local pulse. (b) Effect of repeatedly pulsing a metallic nanotube connected to a Ti/Au electrode. Applying a local pulse of 1 V for a second and third time does not result in any decrease in contact resistance and is similar to the first pulse applied. Applying a 6 V pulse for the second and third time results in a significant increase of the contact resistance, as seen from the plot in panel b.

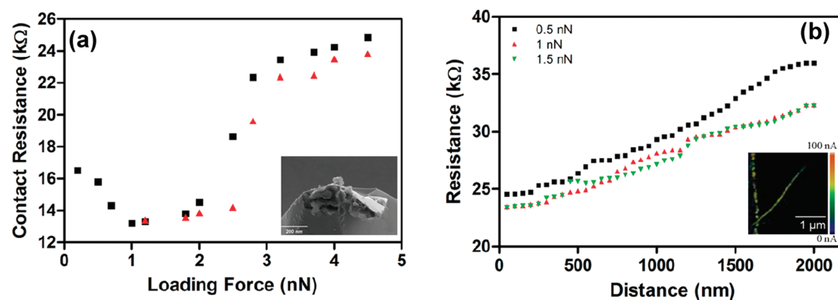

Figure 5. (a) Analysis of the contact resistance between a metallic tube and Pd electrode as a function of loading force while applying a pulsing voltage of 6 V. The contact resistance decreases gradually as the loading force is increased, and the minimum contact resistance is attained around 1 nN, after which the contact resistance increases rapidly (as seen from the black trace) due to tip degradation, as shown in the scanning electron micrograph in the inset. The red trace in the plot results from engaging a new tip at a starting loading force of 1 nN, and the contact resistance is stable until ~2 nN, after which the tip degrades rapidly resulting in higher contact resistance values. (b) Analysis of contact resistance as a function of loading force while scanning over a metallic tube connected to a Pd electrode. The contact resistance decreases slightly by ~1 kΩ on shifting the loading force, while scanning from 0.5 to 1 nN does not change on applying 1.5 nN. Increasing the loading force to 2 nN results in physical damage to the nanotube.

ues plotted in Figure 4a were obtained by tracing the current along a metallic tube (tube diameter = 1.65 nm) connected to the Ti/Au electrode using a bias of 2 mV after applying a local pulse ranging from 1 to 6.5 V. For each case, the duration of the applied voltage pulse was ~2 s. Increasing the pulse duration and decreasing the applied voltage (*e.g.*, 10−60 s at biases of 1−3 V) proved unsuccessful as the metal coating on the tip degraded rapidly for long pulse durations, making the subsequent resistance measurements unreliable. To keep track of this problem, the resistance of the probe tip was constantly measured against a separate reference surface electrode of known resistance.

In order to verify the effect of applying repeated pulses, we selected a metallic tube connected to a Ti/Au electrode and applied voltage pulses ranging from 1 to 6 V and monitored its effect on the overall contact resistance. We observed that applying subsequent pulses from 1 to 3 V did not alter the contact resistance, whereas applying more than 4−6 V resulted in the increase of the contact resistance every time after the pulse was applied (see Supporting Information). The highest increase in contact resistance was measured while applying 6 V on the same tube for the third time, as shown in Figure 4b.

Optimizing the loading force is essential for reliable CI-AFM measurements. The loading force has to be high enough to penetrate the contamination layer between the tip apex and the sample under investigation to establish electrical contact. We analyzed the contact resistance between a metallic nanotube (tube diameter = 1.5 nm) connected to a Pd electrode as a function of loading force while pulsing the electrode at 6 V for 2 s, as shown in Figure 5a (black trace). The contact resistance of the tube was subsequently analyzed at a lower loading force of 0.5 nN with a bias voltage of 4 mV. The contact resistance was observed to gradually decrease as we gently increased the loading force. A minimum contact resistance of ~13 kΩ was obtained when a loading force of ~1 nN was applied. A further increase in loading force resulted in a slight increase in contact resistance followed by an abrupt increase for loading forces above 2 nN. SEM analysis revealed that the abrupt increase is associated with a degradation of the metal-coated tip as shown in the inset in Figure 5a. A new probe used to continue the pulsing experiment (6 V, 2 s) but starting from an initial loading force of 1 nN is shown as the red curve in Figure 5a. Clearly, the result is the same as the original experiment and points to the catastrophic breakdown of the tip at higher loading. To check if the contact had actually improved despite breakdown of the probe, we examined the resistance with a third probe showing a value that corresponds to the minimum value in Figure 5a. These data indicate that contacting the electrode at higher loading force (>2 nN) only results in the degradation of the tip and does not in any way improve the contact resistance. Optimization measurements on metallic/semiconducting nanotubes connected to the Pd electrode showed similar behavior.

In order to ascertain the contribution between the metal-coated tip and the tube to the overall measured resistance, we scanned a metallic nanotube (tube diameter = 1.7 nm) connected to a Pd electrode at varying loading conditions of 0.5, 1, and 1.5 nN. The contact resistance was found to decrease by ~1 kΩ when increasing the loading force from 0.5 to 1 nN, as shown in Figure 5b, but showed no change on increasing the contact force further. Increasing the loading force to 2 nN and above, resulted in the physical damage to the tube. Consequently, throughout the remainder of the study, we used pulsing conditions of 6 V for 2 s under a loading force of ~1 nN to achieve the best contact resistance values.

To compare the effect of the local annealing treatment on the two different metal electrodes used in this study, we performed a statistical analysis of the contact resistance of metallic/semiconducting tubes connected to Pd and Ti/Au electrodes before and after pulsed annealing. We then extracted the mean contact resistance, as shown in Table 1, and for which at least 20 individual tubes were measured in each case. Table 1

TABLE 1. Results from the Statistical Analysis of the Contact Resistance of Pristine/Pulse Annealed Metallic and Semiconducting Tubes Contacted by Ti/Au and Pd Electrodes

	contact resistance (kΩ)			
	metallic		semiconducting	
metal electrode	pristine	annealed	pristine	annealed
Ti/Au	(40 ± 2.5)	(25 ± 2.5)	(105 ± 4.8)	(85 ± 3.6)
Pd	(25 ± 2.5)	(11 ± 1.6)	(54 ± 5.4)	(32 ± 3.1)

shows that the mean contact resistance of a metallic tube connected to Ti/Au decreased by ~15 kΩ after the pulse annealing treatment, while that for a semiconducting tube connected to Ti/Au showed a reduction of ~20 kΩ. The corresponding data for metallic and semiconducting tubes contacted by the Pd electrode before and after the pulse annealing revealed decreases of ~15 and ~22 kΩ, respectively. The optimized values shown in Table 1 are among the lowest contact resistances ever reported.

To determine whether this pulse annealing treatment resulted in a permanent enhancement, we investigated the stability of the contacts over time, as shown in Figure 6. The optimized Pd contacts did not vary by more than 5% during a five month period, which can be largely ascribed to changes in the scanning conditions caused by the use of different metallic-coated tips. Moreover, Pd contacts that were improved by using suboptimal pulse conditions retained the same contact resistance over time, indicating that it is possible to tune the contact resistance at any level between the initial and optimized levels. In contrast, we found a steady increase in the contact resistance for tubes connected to the Ti/Au electrode regardless of whether the contacts were optimized (see Figure 6).

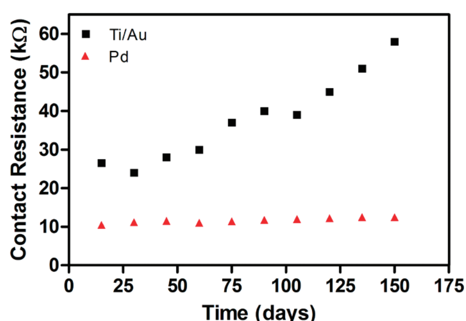

Figure 6. Analysis of contact resistance as a function of time for metallic nanotubes contacted by a Ti/Au electrode (black curve) and Pd electrode (red curve). The contact resistance was found to increase for metallic annealed nanotubes contacted by the Ti/Au electrode when measured periodically over a time period of 150 days. In contrast, we did not measure any significant change in the contact resistance of the Pd contacted metallic annealed tube over the same time period.

CONCLUSION

There are several important outcomes from this work. First, Pd electrodes are superior to Ti/Au independent of the electronic nature of the nanotube. This is consistent with previous literature results[1,2,20] and has been attributed to better wetting properties of the Pd contacts and, in the case of semiconducting tubes, a larger work function (5.12 *vs* 4.33 eV) that minimizes the influence of Schottky barrier formation. The optimized contact resistance measured for metallic nanotubes contacted by a Pd electrode as a result of local pulsed annealing was ~11 kΩ and comparable range to previously reported values of ~15 kΩ reported by Javey *et al.*[1] (tube diameter = ~2 nm) but much lower that the of ~100 kΩ reported by Woo *et al.*[13] (tube diameter = ~0.8 nm), who used a pulse annealing method where the current was passed along the entire metal electrode. This shows the advantages of our CI-AFM pulse technique and may indicate that the application of a local force is important to help optimize the contact. We speculate that the combination of Joule heating and pressure is important in assisting in the formation of chemical bonds for achieving good electrical contacts. Significantly, we find that optimized semiconductor nanotube contacts with Ti/Au resulted in a much smaller decrease in contact resistance (15%) compared to Pd (45%), the latter yielding values that are only a factor of 3 larger than the very best contacts with metallic tubes (33 *vs* 11 kΩ). These results show that the optimization process leads to an effective collapse of the Schottky barrier so that it is possible to tunnel through the remnant barrier with minimum resistance.

The enhanced performance of Pd is likely due to the better band alignment given its larger work function and the fact that the present tubes are p-type doped (see Figure 1). The stability of the Pd contacts is also striking compared to Ti/Au. The Joule heating associated with the optimization process may also promote specific chemical bonding interactions that have been predicted between Pd and carbon nanotubes.[13] The noble character and enhanced wetting properties of Pd on nanotubes make it very resistive to oxidation.

In contrast, Ti is chemically more reactive in air, and even the deposited 20 nm of gold on top of the Ti layer, which is typical in Ti device contacts, cannot prevent slow oxidation and the deterioration of the contact.

EXPERIMENTAL SECTION

SWCNTs synthesized by arc discharge technique (Iljin Nanotech arc discharge tubes) were dispersed in *N*-methylpyrrolidone (NMP), an organic solvent that has been shown before to successfully exfoliate carbon nanotubes in the liquid phase.[21,22] The nanotube dispersions were spray coated onto silicon dioxide substrates (300 nm oxide thickness) and patterned by standard UV-lithography techniques. The metal (Pd and Ti/Au) was thermally evaporated onto the patterned silicon dioxide substrates, and the thickness of the metal in each case was ~25 nm. In the case of Ti/Au, Ti (5 nm) was used as a good adhesion layer after which 20 nm of Au was deposited. The samples were then sub-

jected to controlled annealing (500 °C for 5 h under argon gas) in order to remove the NMP molecules adsorbed on the tubes and on the respective metal electrodes. CI-AFM (operated on Dimension V AFM) is a nondestructive, two-contact measurement in which a metal-coated AFM probe (Cr/Pt, 0.2 N/m, Cont E, Budget Sensors) acts as a mobile contact capable of addressing and measuring currents at specific locations within the sample.

In this technique, a bias is applied to the substrate electrode or the tip, and the latter is brought into contact and scanned over the nanotubes connected to the electrode, while the current and topography data are recorded. In addition, it is possible to discriminate between and selectively analyze metallic and semiconducting tubes within the sample by applying a gate voltage. The application of a backgate (silicon wafer acts as the gate electrode) voltage sweeps carriers from the semiconducting tubes, thereby turning them off in CI-AFM images, such that only the remaining metallic tubes are visible. All of the CI-AFM measurements were carried out with clean metal-coated tips as tip contamination leads to higher contact resistance between the tip and the measured sample. To ensure that this is indeed the case, the contact resistance between the metal-coated tip and the electrode was monitored between scans, yielding values of ~400 and ~100 ohms for the Ti/Au and Pd electrodes, respectively.

Acknowledgment. We acknowledge the Science Foundation Ireland funded Principle Investigator Award (Grant No. 06/IN.1/I106) and the Science Foundation Ireland funded collaboration (SFI Grant 03/CE3/M406s1) between Trinity College Dublin, University College Cork, and Hewlett-Packard, Dublin Inkjet Manufacturing Operation which allowed this work to take place.

Supporting Information Available: Results of the influence of repeated pulsing experiment on the contact resistance and the details of the influence of the tip lifetime on the overall quality of the conductance images is provided. The experiments conducted with a larger probe on reducing the contact resistance are also been discussed in the Supporting Information. This material is available free of charge *via* the Internet at http://pubs.acs.org.

REFERENCES AND NOTES

1. Javey, A.; Guo, J.; Paulsson, M.; Wang, Q.; Mann, D.; Lundstrom, M.; Dai, H. High-Field Quasiballistic Transport in Short Carbon Nanotubes. *Phys. Rev. Lett.* **2004**, *92*, 106804-4.
2. Javey, A.; Guo, J.; Wang, Q.; Lundstrom, M.; Dai, H. Ballistic Carbon Nanotube Field-Effect Transistors. *Nature* **2003**, *424*, 654–657.
3. Javey, A.; Guo, J.; Farmer, D. B.; Wang, Q.; Wang, D.; Gordon, R. G.; Lundstrom, M.; Dai, H. Carbon Nanotube Field-Effect Transistors with Integrated Ohmic Contacts and High K Gate Dielectrics. *Nano Lett.* **2004**, *4*, 447–450.
4. Kane, A. A.; Sheps, T.; Branigan, E. T.; Apkarian, V. A.; Cheng, M. H.; Hemminger, J. C.; Hunt, S. R.; Collins, P. G. Graphitic Electrical Contacts to Metallic Single-Walled Carbon Nanotubes Using Pt Electrodes. *Nano Lett.* **2009**, *9*, 3586–3591.
5. Zhang, Z.; Wang, S.; Ding, L.; Liang, X.; Pei, T.; Shen, J.; Xu, H.; Chen, Q.; Cui, R.; Li, Y.; Peng, L.-M. Self-Aligned Ballistic n-Type Single-Walled Carbon Nanotube Field-Effect Transistors with Adjustable Threshold Voltage. *Nano Lett.* **2008**, *8*, 3696–3701.
6. Ding, L.; Wang, S.; Zhang, Z.; Zeng, Q.; Wang, Z.; Pei, T.; Yang, L.; Liang, X.; Shen, J.; Chen, Q.; Cui, R.; Li, Y.; Peng, L.-M. Y-Contacted High-Performance n-Type Single-Walled Carbon Nanotube Field-Effect Transistors: Scaling and Comparison with Sc-Contacted Devices. *Nano Lett.* **2009**, *9*, 4209–4214.
7. Marty, L.; Bouchiat, V.; Naud, C.; Chaumont, M.; Fournier, T.; Bonnot, A. M. Schottky Barriers and Coulomb Blockade in Self-Assembled Carbon Nanotube FETs. *Nano Lett.* **2003**, *3*, 1115–1118.
8. Lee, J.-O.; Park, C.; Kim, J.-J.; Kim, J.; Park, J. W.; Yoo, K.-H. Formation of Low-Resistance Ohmic Contacts between Carbon Nanotube and Metal Electrodes by a Rapid Thermal Annealing Method. *J. Phys. D: Appl. Phys.* **2000**, *33*, 1953–1956.
9. Seidel, R.; Liebau, M.; Duesberg, G. S.; Kreupl, F.; Unger, E.; Graham, A. P.; Hoenlein, W.; Pompe, W. *In-Situ* Contacted Single-Walled Carbon Nanotubes and Contact Improvement by Electroless Deposition. *Nano Lett.* **2003**, *3*, 965–968.
10. Chen, C.; Yan, L.; Kong, E. S.-W.; Zhang, Y. Ultrasonic Nanowelding of Carbon Nanotubes to Metal Electrodes. *Nanotechnology* **2006**, *17*, 2192–2197.
11. Chen, Q.; Wang, S.; Peng, L.-M. Establishing Ohmic Contacts for *In Situ* Current and Voltage Characteristic Measurements on a Carbon Nanotube Inside the Scanning Electron Microscope. *Nanotechnology* **2006**, *17*, 1087–1098.
12. Dong, L.; Youkey, S.; Bush, J.; Jiao, J.; Dubin, V. M.; Chebiam, R. V. Effects of Local Joule Heating on the Reduction of Contact Resistance between Carbon Nanotubes and Metal Electrodes. *J. Appl. Phys.* **2007**, *101*, 024320-7.
13. Woo, Y.; Duesberg, G. S.; Roth, S. Reduced Contact Resistance between an Individual Single-Walled Carbon Nanotube and a Metal Electrode by a Local Point Annealing. *Nanotechnology* **2007**, *18*, 095203-7.
14. Garg, A.; Sinnott, S. B. Effect of Chemical Functionalization on the Mechanical Properties of Carbon Nanotubes. *Chem. Phys. Lett.* **1998**, *295*, 273–278.
15. Nirmalraj, P. N.; Lyons, P. E.; De, S.; Coleman, J. N.; Boland, J. J. Electrical Connectivity in Single-Walled Carbon Nanotube Networks. *Nano Lett.* **2009**, *9*, 3890–3895.
16. Stadermann, M.; Papadakis, S. J.; Falvo, M. R.; Novak, J.; Snow, E.; Fu, Q.; Liu, J.; Fridman, Y.; Boland, J. J.; Superfine, R.; Washburn, S. Nanoscale Study of Conduction through Carbon Nanotube Networks. *Phys. Rev. B* **2004**, *69*, 201402.
17. Li, S.; Yu, Z.; Rutherglen, C.; Burke, P. J. Electrical Properties of 0.4 cm Long Single-Walled Carbon Nanotubes. *Nano Lett.* **2004**, *4*, 2003–2007.
18. Yao, Z.; Kane, C. L.; Dekker, C. High-Field Electrical Transport in Single-Wall Carbon Nanotubes. *Phys. Rev. Lett.* **2000**, *84*, 2941–2944.
19. Yao, Z.; Postma, H. W. C.; Balents, L.; Dekker, C. Carbon Nanotube Intramolecular Junctions. *Nature* **1999**, *402*, 273–276.
20. Tersoff, J. Nanotechnology: A Barrier Falls. *Nature* **2003**, *424*, 622–623.
21. Ausman, K. D.; Piner, R.; Lourie, O.; Ruoff, R. S.; Korobov, M. Organic Solvent Dispersions of Single-Walled Carbon Nanotubes: Toward Solutions of Pristine Nanotubes. *J. Phys. Chem. B* **2000**, *104*, 8911–8915.
22. Giordani, S.; Bergin, S. D.; Nicolosi, V.; Lebedkin, S.; Kappes, M. M.; Blau, W. J.; Coleman, J. N. Debundling of Single-Walled Nanotubes by Dilution: Observation of Large Populations of Individual Nanotubes in Amide Solvent Dispersions. *J. Phys. Chem. B* **2006**, *110*, 15708–15718.